Nuclear Science and Techniques (2022) 33:165
https://doi.org/10.1007/s41365-022-01141-8

Evaluating the JEFF 3.1, ENDF/B-VII.0, JENDL 3.3, and JENDL 4.0 nuclear data libraries for a small 100 MWe molten salt reactor with plutonium fuel

Cici Wulandari[1] · Abdul Waris[2,3] · Sidik Permana[2,3] · Syeilendra Pramuditya[2,3]

Received: 8 February 2022 / Revised: 11 September 2022 / Accepted: 26 September 2022 / Published online: 16 December 2022
© The Author(s), under exclusive licence to China Science Publishing & Media Ltd. (Science Press), Shanghai Institute of Applied Physics, the Chinese Academy of Sciences, Chinese Nuclear Society 2022

Abstract
This study evaluated the nuclear data libraries for a small 100 Mega Watt electric (MWe) Molten Salt Reactor with plutonium fuel. The reactor has a power output of 100 MWe, which meets the demand for electricity generation in several regions or provinces outside Java Island. Several nuclear data libraries, such as JEFF 3.1, ENDF/B-VII.0, JENDL 3.3, and JENDL 4.0, were used for a more comprehensive evaluation. LiF–BeF_2–ThF_4–PuF_4 was used as the initial fuel composition. The thorium and plutonium concentrations in the fuel salt were varied to obtain the optimum fuel composition, leading to critical conditions. The results showed some neutronic parameters, such as the conversion ratio, neutron spectra, and effective multiplication factors, from three different nuclear data libraries. By changing the plutonium concentration in the initial fuel salt composition, the minimum plutonium loaded for the reactor criticality during 2000 days of operation time was determined to be 0.995, 0.91, 0.87, and 0.90 mol% for JEFF 3.1, ENDF/B-VII.0, JENDL 3.3, and JENDL 4.0, respectively. The differences in the values of each parameter were due to several factors, such as the cross-section values and number of nuclides in the nuclear data libraries. Several safety parameters were also investigated to ensure the possibility of utilizing PuF_4 in the reactor.

Keywords Neutronics · Plutonium · Small MSR · Thorium · SRAC

1 Introduction

Indonesia is an archipelago country with various islands of different sizes, but they are mostly small. The energy demand on these islands is relatively low, approximately 100 MWe, owing to their low populations. However, electricity transmission from large islands to small islands is not yet possible. Therefore, a small nuclear reactor is needed to meet the energy demand of developing areas, such as those in several regions or provinces in Indonesia outside of Java Island, of approximately 100 MWe. This would also allow the reduction in carbon emissions to help address climate change.

One of the reactor types that can generate small power outputs is the Molten Salt Reactor (MSR). The MSR is a type of Generation IV nuclear power technology that uses molten salt as fuel. Dissolved salt is mixed with fission products, and actinides circulate through the active core to the primary heat exchanger [1]. Based on graphite moderator utilization, this reactor can be operated in the

The authors acknowledge the Institut Teknologi Bandung Research Grant and the Ministry of Research Technology and Higher Education of the Republic of Indonesia for supporting this research activity and publication.

✉ Abdul Waris
awaris@itb.ac.id

1 Department of Physics, Faculty of Mathematics and Natural Sciences, Institut Teknologi Bandung, Bandung 40132, Indonesia

2 Nuclear Physics and Biophysics Research Division, Department of Physics, Faculty of Mathematics and Natural Sciences, Institut Teknologi Bandung, Bandung 40132, Indonesia

3 Department of Nuclear Science and Engineering, Faculty of Mathematics and Natural Sciences, Institut Teknologi Bandung, Jl. Ganesa 10, Bandung 40132, Indonesia

thermal, epithermal, and fast neutron spectra. Moreover, this reactor was designed using advanced systems in terms of inherent safety, proliferation resistance, energy sustainability, and waste burning. These systems are potentially interesting for the development and research of MSR technology.

The Oak Ridge National Laboratory pioneered MSR concepts, such as the aircraft reactor experiment [2, 3], MSR experiment [4], and molten salt breeder reactor [5]. These projects described the basic concept of MSR technology, including a re-evaluation of reactor performance and the development of other systems, such as waste burning and fuel reprocessing [6, 7]. In addition, the concept of thorium molten salt nuclear energy synergetics (THORIMS-NES) [8, 9] has recently been studied in Japan for several MSR types with different power outputs. The FUJI-U3 reactor [10, 11] is a THORIMS-NES concept with a power output of 200 MWe that uses $^{233}U/^{232}Th$ as the primary fuel. Because the power output in the FUJI reactor can be adjusted, there is a high probability of it being designed for a small reactor.

The FUJI-Pu reactor [12] is one of the reactor types developed using the THORIMNES concept. Some plutonium isotopes were considered to be the starting fuel in this reactor. The goal was to replace ^{233}U as an initial fissile used in other FUJI reactor concepts, such as FUJI-12, FUJI-II, and FUJI-U3. FUJI-Pu is a 1- and 2-region [13] reactor core with a high neutron flux at the center of the core. The neutron flux distribution is an important parameter because it is related to the reactor safety system and fission intensity in the reactor [14]. The design of a 3-region core was introduced to provide flattening neutron flux in the reactor core [10]. Therefore, a small MSR should adopt the design of the 3-region core concept and the utilization of plutonium as an initial fuel.

In our previous study, the neutronic performances of FUJI MSR using plutonium fuel [15] and plutonium/minor-actinide fuel [16–18] were evaluated using the standard reactor analysis code (SRAC (Ver. 2002)), which was established by the Japan Atomic Energy Research Institute using the nuclear data library JENDL 3.2 [19]. However, the nuclear data library utilized in previous studies is outdated, and newer versions, such as JENDL 3.3 [20] and JENDL 4.0 [21], are currently available.

This study investigated the optimization of plutonium fuel loading on the neutronic performance of a small 100 MWe MSR. The initial fuel salt composition used was $LiF–BeF_2–ThF_4–PuF_4$. Several plutonium isotopes employed in PuF_4, such as ^{238}Pu, ^{239}Pu, ^{240}Pu, ^{241}Pu, and ^{242}Pu. The plutonium isotope with odd mass numbers was utilized as a fissile material. At the same time, the plutonium isotope with even mass numbers and ^{232}Th was used as a fertile material. Based on a previous study, this fuel scheme is feasible for producing ^{233}U with Th/Pu as the starting fuel [22], which leads to achieving sustainable energy from thorium utilization in the MSR [23–25].

This study aimed to obtain the minimum required PuF_4 fuel concentration for 2000 days of reactor operation without a refueling scheme by varying the plutonium concentration in the initial fuel salt. It was assumed that on day 2001, chemical processing of the fuel salt would be performed, which is based on the FUJI-U3 reactor study [10]. The utilization of plutonium in fuel salts aimed to burn weapons-grade plutonium (WGPu) [26, 27] in the MSR and reduce the risk of nuclear proliferation [28]. Although this scenario is only intended for theoretical research, the utilization of WGPu as a fuel in MSR is very promising in terms of energy resources, radiation level, and heat generation.

Moreover, several nuclear data libraries, such as JEFF 3.1 [29], ENDF/B-VII.0 [30], JENDL 3.3, and JENDL 4.0, were employed to provide information on trans-plutonium sensitivity and to show the neutronic parameter dependence on nuclear data libraries. JENDL 3.3 and JENDL 4.0 were compared to obtain the neutronic parameter sensitivity in small MSR based on the evaluation of the two libraries. JENDL 3.3 is reported to have overestimated cross-section values for some nuclides compared to JENDL 4.0. To compare trans-plutonium, the JENDL, ENDF, and JEFF libraries were compared. In addition, the effect of the plutonium concentration on some neutronic parameters, such as the neutron spectra, conversion ratio (CR), and effective multiplication factor, was analyzed in this study. Moreover, a safety analysis was also considered, such as the moderator temperature coefficient (MTC), Doppler reactivity coefficient (DRC), and control rod worth (CRW), to show the possibility of plutonium utilization in the reactor.

2 Reactor specification

Table 1 lists the small 100 MWe MSR parameters adopted from the FUJI-U3 reactor [10]. However, in this study, the power output of the reactor was half that of FUJI-U3. It is considered to meet the energy demand of small islands in Indonesia (approximately 100 MWe). The geometry of the active core was a cylinder consisting of several hexagonal graphite layers and a cylindrical fuel channel. The reactor was equipped with a graphite moderator with a density of 1.8 g/cm^3 that can slow down neutrons to the thermal energy region. The lifespan of the graphite moderator was related to the neutron irradiation process during reactor operation [31]. The fuel used was thorium-WGPu with eutectic fluoride salts of lithium and beryllium [32] as the heat transfer media from the active core to the secondary loop.

Figure 1 shows the small MSR active core design divided into three regions with different fuel volume fractions. Previous studies numerically showed that the flattening of the

Table 1 The parameters of a small 100 MWe Molten Salt Reactor

Reactor parameter	Specification
Power output (thermal)	250 MWTh
Power output (electric)	100 MWe
Thermal efficiency	40%
Operation time	2000 days
Initial fuel composition	$LiF–BeF_2–ThF_4–PuF_4$
Temperature fuel salt (in/out)	833/973 K
Core	
Fuel volume fraction (av.)	36%
Diameter/height	4.72/4.66 m
Fuel path/duct	
Fuel volume fraction	90 vol%
Width	0.04 m
Reflector	
Fuel volume fraction	0.5 vol%
Thickness	0.30 m

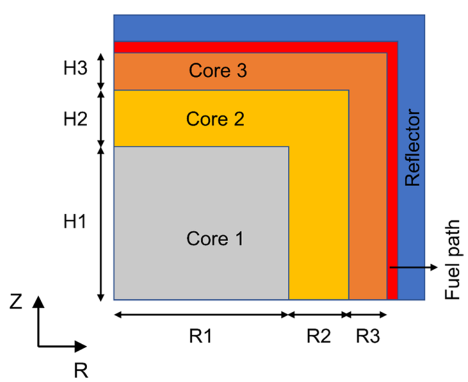

Fig. 1 (Color online) The core configuration in the radial and axial direction with one-fourth of the active core

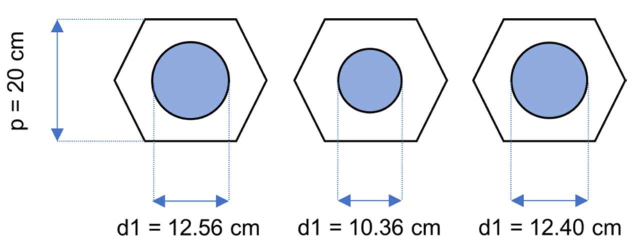

Fig. 2 The layout of hexagonal graphite and the cylindrical fuel channel for different core regions

neutron flux distribution and graphite lifespan could be enhanced by varying the fuel volume fraction in the active core [33, 34]. Therefore, the excessive reactivity at one point in the active core can be avoided. In addition, different fuel volume fractions affect the size of the fuel channel. Figure 2 shows the layout of hexagonal graphite and cylindrical fuel channels for different core regions. In this study, the side-to-side length (*p*) of hexagonal graphite was 20 cm, and the diameters of the fuel channel were 12.56, 10.36, and 12.40 cm for the Core 1 (*d*1), Core 2 (*d*2), and Core 3 (*d*3) regions, respectively (Table 2).

3 Calculation methods

In this study, variations in the fuel salt composition were employed to obtain the reactor criticality, which is provided in Tables 3, 4, 5, and 6 for JENDL 3.3, JENDL 4.0, ENDF/B-VII.0, and JEFF 3.1, respectively. The percentage concentration of both LiF and BeF_2 was fixed at 72 and 16 mol%, respectively, while the total percentage concentration of ThF_4 and PuF_4 was 12 mol%. The percentage PuF_4 concentration to the total percentage ThF_4 and PuF_4 concentration was varied to achieve reactor criticality. The WGPu isotopic compositions [26] are presented in Table 7.

The neutronic performance was evaluated using the diffusion method in the SRAC 2006 program code. The SRAC system was designed to perform neutronic aspect calculations for the various reactors. This system can also produce cross-sectional groups (macroscopic and microscopic), fuel channel calculations, core calculations, and burnup analyses. The fuel channel in this study was calculated using the PIJ module of the SRAC 2006 code, which uses a collision probability technique. In the SRAC system, the structure number of the energy group is 107, which is compressed into 30 groups (24 groups of fast neutron energies and six groups of thermal neutron energies) [10]. The geometry of the fuel channel was modeled, as shown in Fig. 2. The fuel channel calculation obtained the macroscopic cross-sectional value for every burnup step. In this study, the burnup step was set to 100 days for 2000 days of reactor operation. These results were used in the core calculations using the CITATION module. The core geometry is shown in Fig. 1 and is divided into 65 radial and 32 axial zones. The fuel and graphite moderators in the core calculation were homogenized to obtain the cross-sectional groups.

This study assumed that the reactor operated continuously for 2000 days without a refueling scheme. If the effective multiplication factor for 2000 days of operation was still below unity, the percentage of PuF_4 was augmented. The calculations were performed using similar parameters for different nuclear data libraries. Several nuclear data libraries were used: JEFF 3.1, ENDF/B-VII.0, JENDL 3.3, and JENDL 4.0. JEFF was created by the European Nuclear Energy Agency, JENDL was established by the Japan Atomic Energy Agency, and ENDF was developed by the US Cross-Section Evaluation Working Group. The year of release and number of nuclides in each nuclear data library are listed in Table 8.

Table 2 Radius, height, and fuel volume fractions of the core regions

	Core 1	Core 2	Core 3
Fuel volume fraction (%)	39	27	45
	Height (cm)		Radius (cm)
H1	123	R1	116
H2	70	R2	80
H3	40	R3	40

Table 3 Variation of the fuel salt composition for JENDL 3.3

LiF (mol%)	BeF_2 (mol%)	ThF_4 (mol%)	PuF_4 (mol%)
72	16	11.30	0.70
		11.25	0.75
		11.20	0.80
		11.13	0.87

Table 4 Variation of the fuel salt composition for JENDL 4.0

LiF (mol%)	BeF_2 (mol%)	ThF_4 (mol%)	PuF_4 (mol%)
72	16	11.30	0.70
		11.25	0.75
		11.20	0.80
		11.15	0.85
		11.10	0.90

Table 5 Variation of the fuel salt composition for ENDF/B-VII.0

LiF (mol%)	BeF_2 (mol%)	ThF_4 (mol%)	PuF_4 (mol%)
72	16	11.30	0.70
		11.25	0.75
		11.20	0.80
		11.15	0.85
		11.09	0.91

Table 6 Variation of the fuel salt composition for JEFF 3.1

LiF (mol%)	BeF_2 (mol%)	ThF_4 (mol%)	PuF_4 (mol%)
72	16	11.30	0.70
		11.25	0.75
		11.20	0.80
		11.15	0.85
		11.10	0.90
		11.05	0.95
		11.005	0.995

Table 7 Weapons-grade plutonium composition for all nuclear data libraries [20]

^{238}Pu	^{239}Pu	^{240}Pu	^{241}Pu	^{242}Pu	^{241}Am
0.01 wt%	93.82 wt%	5.80 wt%	0.13 wt%	0.02 wt%	0.22 wt%

Table 8 Comparisons of the released year and number of nuclides of JENDL 3.3, JENDL 4.0, and JEFF 3.1

Nuclear libraries	JENDL 3.3	JENDL 4.0	ENDF/B-VII.0	JEFF 3.1
Released year	2002	2010	2006	2005
Number of nuclides	337	406	393	381

4 Results and discussion

4.1 Effect of PuF_4 concentration on reactor criticality

The effective multiplication factor (k_{eff}) values as a function of operation time for 0.80% mol of the PuF_4 concentration in the fuel for JENDL 3.3, JENDL 4.0, ENDF/B-VII.0, and JEFF 3.1 are shown in Fig. 3. The trend of the k_{eff} value was similar to that of all cases wherein it decreases during the operation time. This fact is estimated by subtracting the fissile material (^{239}Pu) to maintain fission in the active core. Moreover, the k_{eff} value of the JEFF 3.1 library was the lowest, followed by ENDF/B-VII.0, JENDL 4.0, and JENDL 3.3. Thus, 0.80 mol% loaded PuF_4 concentration is insufficient to maintain the critical condition for 2000 days of operation time for all cases. The calculated critical operation time of the reactor with 0.80 mol% PuF_4 concentration in the fuel for JENDL 3.3, JENDL 4.0, ENDF/B-VII.0, and JEFF 3.1 was 1400, 1300, 1200, and 600 days, respectively.

In general, the above results on the differences in the criticality conditions (k_{eff}) can be analyzed by comparing the total number of nuclides of the three libraries used, as shown in Table 8.

As shown in Table 8, the number of nuclides in each library was diverse. For instance, the JENDL 4.0 library is an updated version of JENDL 3.3, with the number of nuclides changing from 337 to 406. Based on reference, 30 fission products were added to JENDL 4.0, as were several updated cross-section values, such as a neutron capture cross section of ^{232}Th, ^{238}Pu, and ^{241}Am in the thermal energy range [21]. Therefore, the calculation with JENDL 3.3 has an underestimated criticality value compared to that with JENDL 4.0.

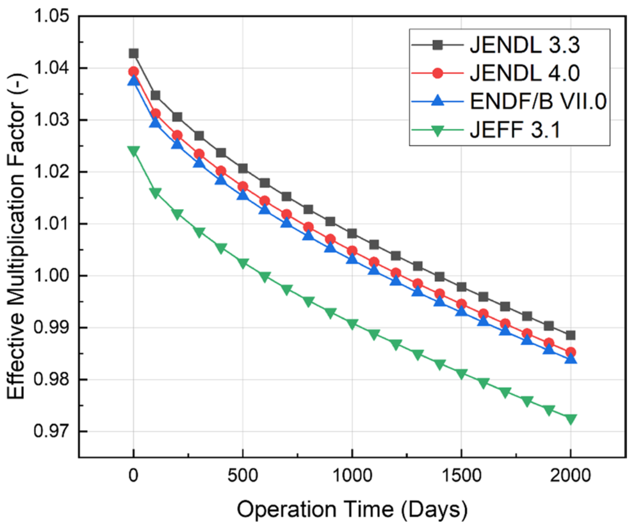

Fig. 3 (Color online) Comparison of k_{eff} values with 0.80 mol% PuF_4 fuel for JENDL 3.3, JENDL 4.0, ENDF/B-VII.0, and JEFF 3.1

Based on the k_{eff} value between ENDF/B-VII.0 and JENDL 4.0, as shown in Fig. 3, the value of ENDF/B-VII was slightly lower than that of JENDL 4.0. The number of nuclides in JENDL 4.0 is greater than that in ENDF/B-VII.0, which can lead to a difference in the k_{eff} value. As shown in Fig. 3, the calculation using JEFF 3.1 had a lower k_{eff} value than that using JENDL 4.0. Even though the number of nuclides on JEFF 3.1 is lower than that on JENDL 4.0. Therefore, it can be predicted that there is an underestimated cross-section value in the JEFF 3.1 calculation compared to the JENDL 4.0 calculation. In addition, the following calculation results and discussion specifically explain the influence of these four libraries on the neutronic performance of a small MSR with plutonium fuel.

The influence of increasing the PuF_4 concentration on the criticality of the reactor is presented in Fig. 4. For JENDL 3.3 in Fig. 4a, PuF_4 concentration varied from 0.70 up to 0.87 mol%, where the k_{eff} value increased as the PuF_4 concentration increased. For JENDL 4.0 in Fig. 4b, the PuF_4 concentration rose from 0.70 up to 0.90 mol%, in which the k_{eff} value trend was similar to JENDL 3.3. For ENDF/B-VII.0 in Fig. 4c, the concentration of PuF_4 varied from 0.70 up to 0.91 mol%. Finally, for JEFF 3.1 in Fig. 4d, PuF_4 concentration varied from 0.70 up to 0.995 mol%, where the k_{eff} trend was also similar to that of the other libraries. Based on the obtained results, the increasing k_{eff} value was parallel to the increasing PuF_4 concentration. This is related to the greater fissile material loaded in the reactor, whose PuF_4 concentrations are presented in Tables 9, 10, 11, and 12 for JENDL 3.3, JENDL 4.0, ENDF/B-VII.0, and JEFF 3.1, respectively. Moreover, as shown in Fig. 16, the addition of PuF_4 increased the hardness of the neutron spectrum. Therefore, the effectiveness of the plutonium fission process was higher because ^{239}Pu is fissile superior in the fast energy region. Therefore, the k_{eff} value obtained was also higher.

As mentioned above, the small MSR was operated for 2000 days without refueling. However, the minimal PuF_4 concentrations in loaded fuel for JENDL 3.3, JENDL 4.0, ENDF/B-VII.0, and JEFF 3.1 were 0.87, 0.90, 0.91, and 0.995 mol%, respectively.

The criticality differences may also have arisen from the different values of the radiative neutron capture cross section of some nuclides in JEFF 3.1, ENDF/B-VII.0, JENDL 3.3, and JENDL 4.0. Figure 5 depicts the radiative neutron capture cross section for important nuclides, such as ^{233}U, ^{232}Th, ^{239}Pu, ^{241}Pu, and ^{241}Am, in the fast, resonance, and thermal energy ranges from these nuclear libraries. Figure 5a shows that the capture cross sections of ^{233}U in these libraries are slightly different in the resonance and fast energy regions. The capture cross section in ENDF/B-VII.0 was the highest, followed by that in JENDL 4.0, JEFF 3.1, and JENDL 3.3. However, the values coincided in the thermal energy range for all nuclear data libraries.

In Fig. 5b, the capture cross sections of ^{232}Th for the four libraries were also different, with the lowest value being for JENDL 4.0 in the resonance and thermal energy range. This means that the probability of the neutron capture process of ^{232}Th for JENDL 4.0 was lower than that for JENDL 3.3 and JEFF 3.1. However, the capture cross section of ^{232}Th in JENDL 4.0 was slightly similar within ENDF/B-VII.0, which could lead to a slight similarity in reactor criticality. In this fuel salt, ^{232}Th was the primary fertile material. Therefore, the neutron capture cross-section differences from the nuclear data libraries can affect ^{233}U production, generating different criticality conditions.

In Fig. 5c, d, the capture cross sections of ^{239}Pu and ^{241}Pu for the four nuclear data libraries had similar conditions to the ^{233}U capture cross section, where the differences were insignificant. However, in the fast energy range, the value for JEFF 3.1 was the highest followed by JENDL 3.3, JENDL 4.0, and ENDF/B-VII.0. The capture cross section of ^{241}Am for all libraries used also had a different value, with the highest value shown in JENDL 4.0, especially in terms of thermal energy, as presented in Fig. 5e. Meanwhile, the JEFF 3.1 trend was similar to that of JENDL 3.3 and ENDF/B-VII.0 in the thermal and fast energy regions. When JENDL 3.3 and JENDL 4.0 were compared, it was found that JENDL 3.3 had an underestimated value of capture cross section, where the number of absorbed neutrons decreased, resulting in a higher k_{eff} value.

The criticality also refers to the microscopic fission cross section, which is described as the fission probability between a neutron and nuclide. Figure 6a–e shows the microscopic fission cross section of a fissile in the reactor. A comparison of the microscopic fission cross sections of ^{233}U for JENDL 3.3, JENDL 4.0, ENDF/B-VII.0, and JEFF

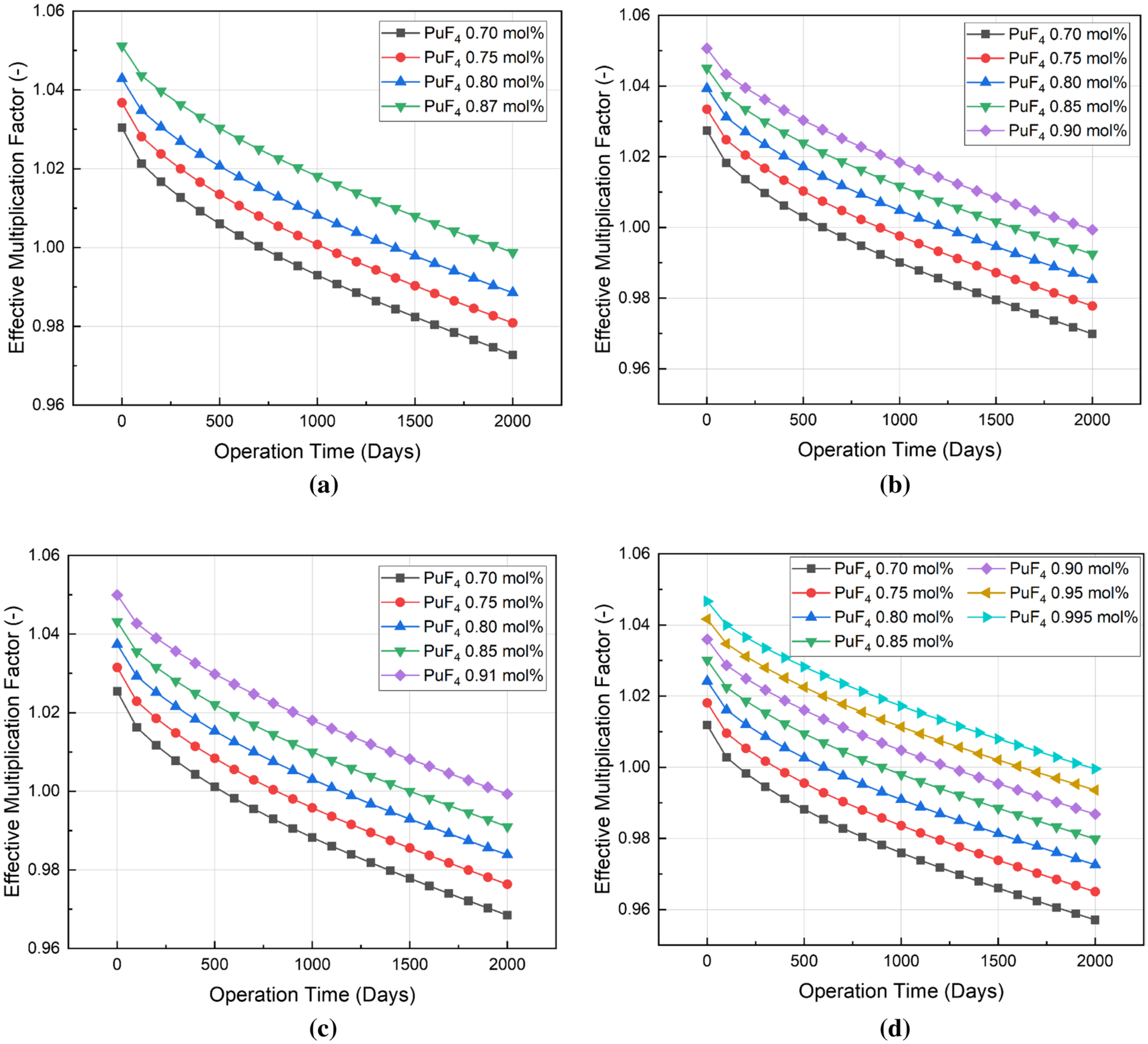

Fig. 4 Comparison of the k_{eff} value with various PuF_4 concentrations for **a** JENDL 3.3, **b** JENDL 4.0, **c** ENDF/B-VII.0, and **d** JEFF 3.1

Table 9 PuF_4 concentration for each plutonium isotope and ^{241}Am with JENDL 3.3

Concentration of PuF_4 (mol%)	$^{238}PuF_4$ (mol%)	$^{239}PuF_4$ (mol%)	$^{240}PuF_4$ (mol%)	$^{241}PuF_4$ (mol%)	$^{242}PuF_4$ (mol%)	$^{241}AmF_4$ (mol%)
0.70	0.00007	0.65674	0.04060	0.00091	0.00014	0.00154
0.75	0.00008	0.70365	0.04350	0.00098	0.00015	0.00165
0.80	0.00008	0.75056	0.04640	0.00104	0.00016	0.00176
0.87	0.00009	0.81623	0.05046	0.00113	0.00017	0.00191

3.1 is shown in Fig. 6a. This shows that the values in the thermal energy region were higher than those in the fast energy region. This indicates that the fission probability of ^{233}U is higher in the thermal energy region, which is suitable for the reactor under consideration. The microscopic fission cross sections of ^{232}Th for the four nuclear data libraries are shown in Fig. 6b. Although ^{232}Th is a fertile material, it still has a fission probability, especially

Table 10 PuF_4 concentration for each plutonium isotope and ^{241}Am with JENDL 4.0

Concentration of PuF_4 (mol%)	$^{238}PuF_4$ (mol%)	$^{239}PuF_4$ (mol%)	$^{240}PuF_4$ (mol%)	$^{241}PuF_4$ (mol%)	$^{242}PuF_4$ (mol%)	$^{241}AmF_4$ (mol%)
0.70	0.00007	0.65674	0.04060	0.00091	0.00014	0.00154
0.75	0.00008	0.70365	0.04350	0.00098	0.00015	0.00165
0.80	0.00008	0.75056	0.04640	0.00104	0.00016	0.00176
0.85	0.00009	0.79747	0.04930	0.00111	0.00017	0.00187
0.90	0.00009	0.84438	0.05220	0.00117	0.00018	0.00198

Table 11 PuF_4 concentration for each plutonium isotope and ^{241}Am with ENDF/B-VII.0

Concentration of PuF_4 (mol%)	$^{238}PuF_4$ (mol%)	$^{239}PuF_4$ (mol%)	$^{240}PuF_4$ (mol%)	$^{241}PuF_4$ (mol%)	$^{242}PuF_4$ (mol%)	$^{241}AmF_4$ (mol%)
0.70	0.00007	0.65674	0.04060	0.00091	0.00014	0.00154
0.75	0.00008	0.70365	0.04350	0.00098	0.00015	0.00165
0.80	0.00008	0.75056	0.04640	0.00104	0.00016	0.00176
0.85	0.00009	0.79747	0.04930	0.00111	0.00017	0.00187
0.91	0.00009	0.85376	0.05278	0.00118	0.00018	0.00200

Table 12 PuF_4 concentration for each plutonium isotope and ^{241}Am with JEFF 3.1

Concentration of PuF_4 (mol%)	$^{238}PuF_4$ (mol%)	$^{239}PuF_4$ (mol%)	$^{240}PuF_4$ (mol%)	$^{241}PuF_4$ (mol%)	$^{242}PuF_4$ (mol%)	$^{241}AmF_4$ (mol%)
0.70	0.00007	0.65674	0.04060	0.00091	0.00014	0.00154
0.75	0.00008	0.70365	0.04350	0.00098	0.00015	0.00165
0.80	0.00008	0.75056	0.04640	0.00104	0.00016	0.00176
0.85	0.00009	0.79747	0.04930	0.00111	0.00017	0.00187
0.90	0.00009	0.84438	0.05220	0.00117	0.00018	0.00198
0.95	0.00010	0.89129	0.05510	0.00124	0.00019	0.00209
0.995	0.00010	0.93351	0.05771	0.00129	0.00020	0.00219

in the fast energy region. JENDL 3.3 and JENDL 4.0, produce fission cross-section values of ^{232}Th in all energy ranges, while JEFF 3.1 and ENDF/B-VII.0 only produce values in the fast energy range. Although the value is relatively low, this discrepancy can lead to differences in the obtained k_{eff} values. The fissionability of ^{232}Th in the JEFF library is only considered in the fast energy region, whereas the JENDL library is considered in all energy ranges. Therefore, the JEFF and ENDF/B-VII.0 library will have a lower k_{eff} value than the JENDL library, as shown in Fig. 3.

As the primary fissile material in this reactor, the microscopic fission cross section of ^{239}Pu for all libraries used is shown in Fig. 6c. The microscopic fission cross sections of ^{239}Pu for JEFF 3.1 and JENDL 3.3 are slightly different in the resonance and fast energy ranges. Similar to ^{239}Pu, the microscopic fission cross section of ^{241}Pu for different nuclear data libraries is presented in Fig. 6d, where the value difference is insignificant. The microscopic fission cross section of ^{241}Am is shown in Fig. 6e. In the thermal energy range, JENDL 4.0 is first, followed by ENDF/B-VII.0, JENDL 3.3, and JEFF 3.1. Again, the values are slightly different for the four nuclear data libraries, which results in a discrepancy in the criticality conditions.

4.2 Effect of PuF_4 concentration on conversion capability

The conversion capability of the reactor is described by the CR value. It is defined as the ratio of the generated fissile to the consumed fissile in the reactor core, and it also represents the reactor performance in terms of sustainable fuel supply. When CR > 1.0, the reactor has a breeding capability. The conversion process of fertile materials can generate fissile materials through neutron capture. Figure 7 shows the conversion capability of the reactor for different nuclear data

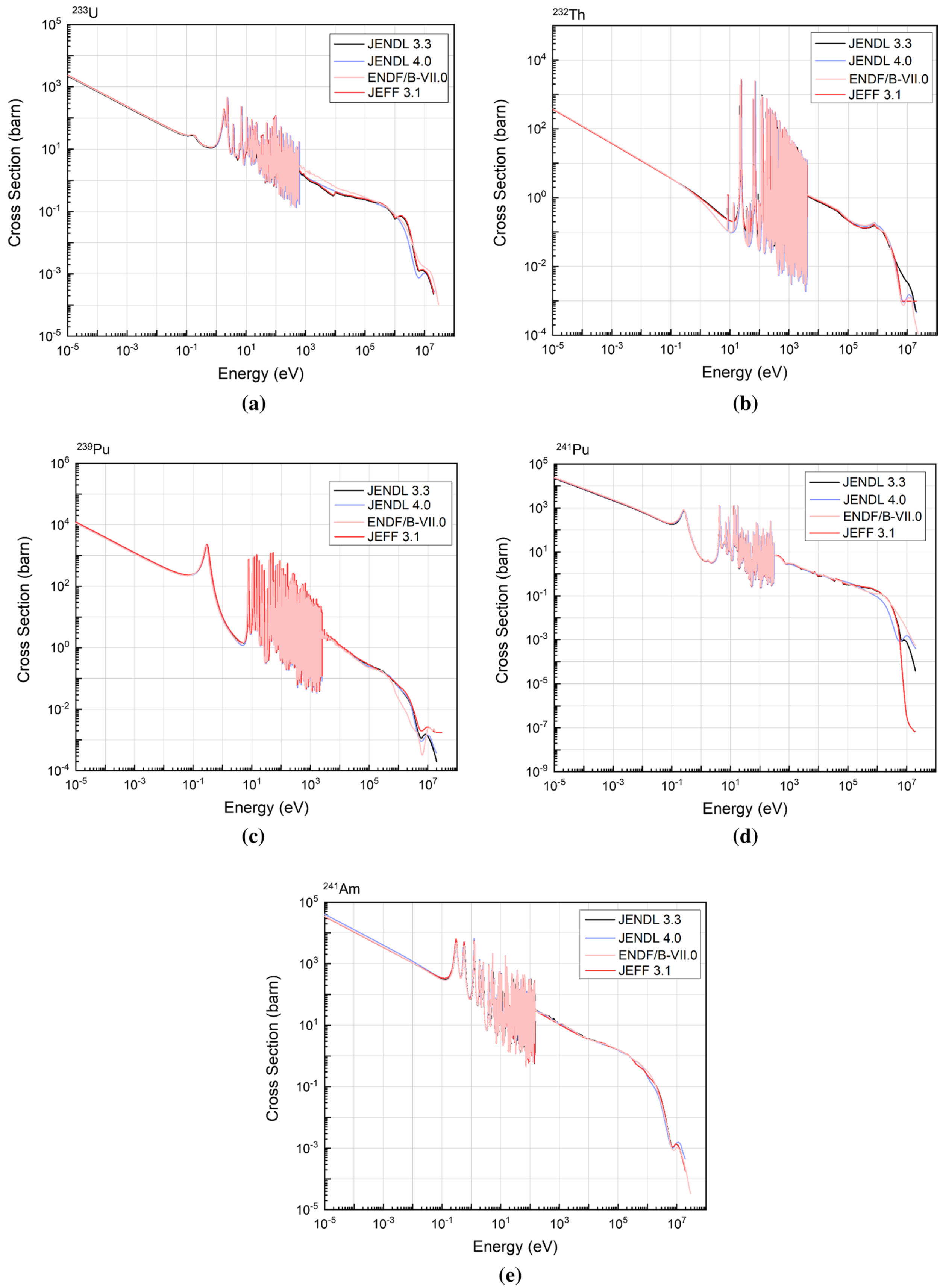

Fig. 5 Radiative neutron capture cross sections of **a** ^{233}U, **b** ^{232}Th, **c** ^{239}Pu, **d** ^{241}Pu, and **e** ^{241}Am

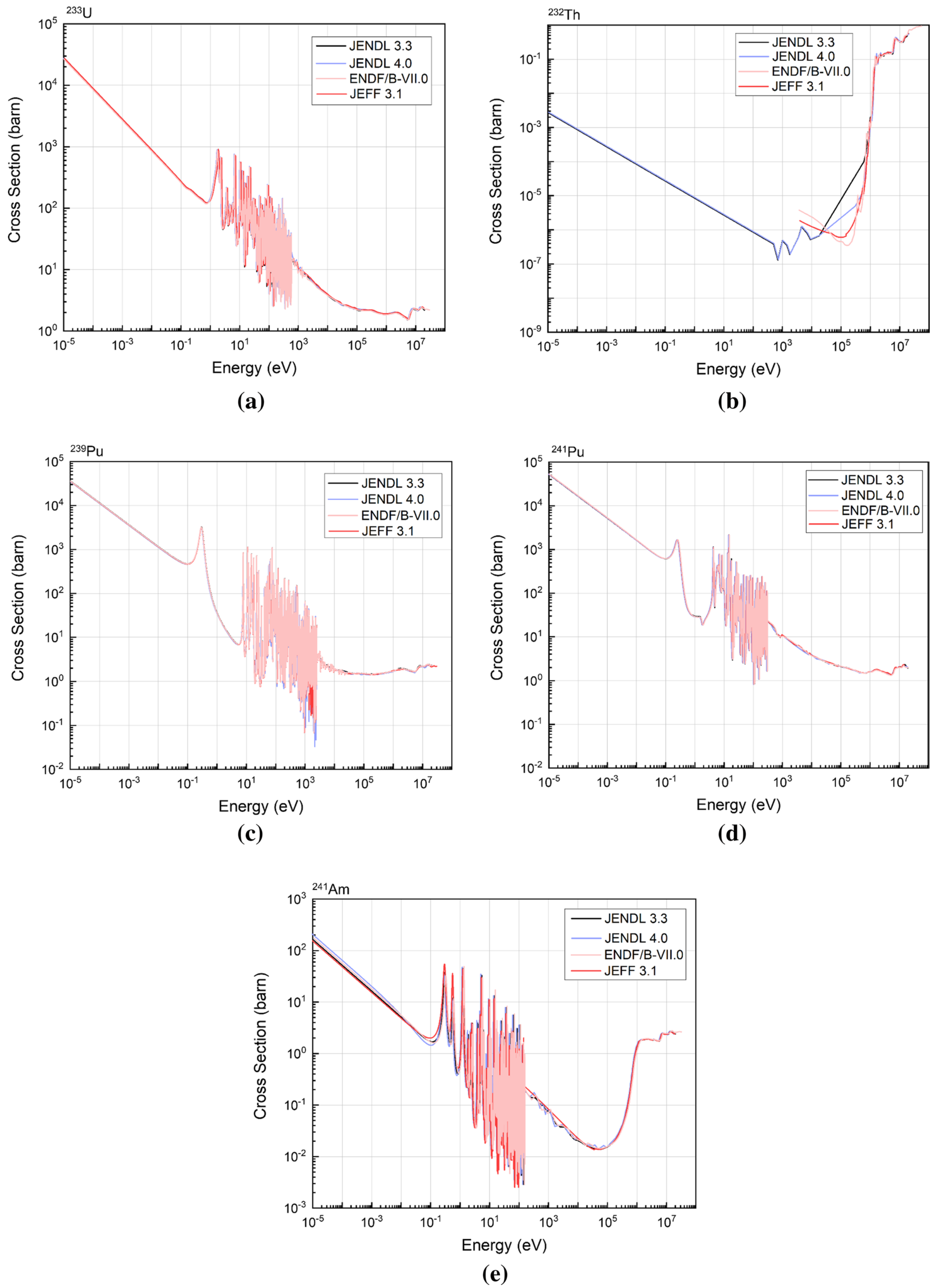

Fig. 6 (Color online) Fission cross sections of **a** ^{233}U, **b** ^{232}Th, **c** ^{239}Pu, **d** ^{241}Pu, and **e** ^{241}Am

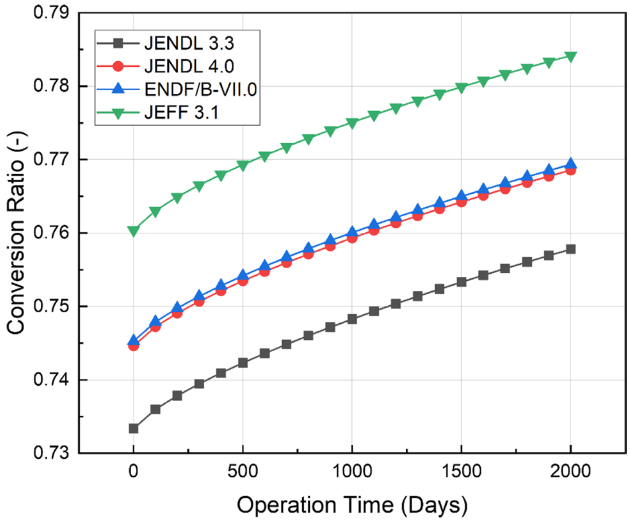

Fig. 7 (Color online) The conversion ratio of 0.80 mol% WGPu fuel with JENDL 3.3, JENDL 4.0, ENDF/B-VII.0, and JEFF 3.1

libraries. The results indicate that the CR trends of JENDL 3.3, JENDL 4.0, ENDF/B-VII.0, and JEFF 3.1 are similar in that the value increases with an increase in the reactor operation time. This shows that the amount of converted fertile material increases during the operation time, as well as fissile material production. The increasing CR is estimated from the contribution of the transmutation of ^{2132}Th and plutonium isotopes with even mass numbers, such as ^{238}Pu, ^{240}Pu, and ^{242}Pu, in the fuel salt. For instance, ^{233}U can be produced through the neutron capture process of ^{232}Th, and ^{239}Pu can be generated from a nuclear reaction similar to that of ^{238}Pu. Based on the data, the CR of 0.80 mol% PuF_4 for all libraries used is different, with that for JEFF 3.1 being 1.94%, 2.04%, and 3.46% higher than that for ENDF/B-VII.0, JENDL 4.0, and JENDL 3.3, respectively.

The difference in the CR values in the four nuclide data libraries can be caused by differences in the number of nuclides and cross-section values in each library. For instance, ^{232}Th is the main fertile material in the reactors. The neutron capture cross section of ^{232}Th in the JEFF 3.1 library is highest compared to that in the ENDF/B-VII.0 and JENDL libraries. Hence, it can cause the CR value in JEFF 3.1 to be higher than that in other libraries. Meanwhile, in both JENDL libraries, the neutron capture cross section of ^{232}Th at JENDL 3.3 is higher than that of JENDL 4.0. However, the CR value of the JENDL 3.3 library was lower than that of the JENDL 4.0, library. This could be due to the neutron capture cross-section factor of other nuclides, as shown in Fig. 5e, which shows that the neutron capture cross section of ^{241}Am of JENDL 4.0 is higher than that of JENDL 3.3.

Moreover, regarding the radiative neutron capture cross section of nuclear data libraries, some heavy nuclides should be discussed, for example ^{233} Pa, which is produced from a capture reaction between ^{232}Th and neutrons. The capture cross section of ^{233} Pa in the JENDL 4.0 library was higher than that in JEFF 3.1, ENDF/B-VII.0, and JENDL 3.3, especially in the thermal energy range. Additionally, the capture cross section of ^{241}Am in the JENDL 4.0 library was the highest, as shown in Fig. 5e. ^{233} Pa and ^{241}Am are heavy nuclides in the reactor that can absorb neutrons and reduce the neutron population. In addition, the capture cross-section difference of plutonium isotopes with even mass numbers was not significant between the three nuclear data libraries, and only ^{240}Pu had a high value in JEFF 3.1. Moreover, the differences were not substantially affected by the CR because of the low concentration of ^{240}Pu in the molten salt.

The influence of the PuF_4 concentration on the conversion capability is shown in Fig. 8 for (a) JENDL 3.3, (b) JENDL 4.0, (c) ENDF/B-VII.0, and (d) JEFF 3.1. These data indicate that the CR trend is almost the same for all nuclear data libraries, which decreases as the PuF_4 concentration increases. Increasing the PuF_4 concentration in the fuel salt affects the ThF_4 concentration, which balances the fuel salt composition. The ThF_4 concentration diminishes with increasing PuF_4 concentration (see Tables 4, 5, 6, and 7 for JENDL 3.3, JENDL 4.0, ENDF/B-VII.0, and JEFF 3.1, respectively. As the primary fertile material in fuel, thorium plays an important role in adjusting the breeding capability of the reactor. This is due to the high absorption cross section of ^{232}Th in the thermal energy range. Therefore, a higher Th concentration in the reactor core augments the CR.

Furthermore, increasing PuF_4 in the fuel salt also increases the concentration of some even mass number plutonium isotopes. In this case, the percentage isotopic composition of plutonium isotopes with even mass numbers was smaller than that of plutonium isotopes with odd mass numbers. Therefore, the conversion capability was not significantly affected by the conversion of plutonium isotopes, even with mass numbers. However, the conversion capability is mainly contributed to by Th conversion in the fuel salt. For instance, as shown in Fig. 9, the atomic density change of ^{232}Th with JEFF 3.1 is the highest, followed by that with JENDL 4.0, ENDF/B-VII.0, and JENDL 3.3.

Figure 10 shows the change in the ^{238}Pu atomic density for different nuclear data libraries, which increased during the operating period. The changes in the JENDL 4.0 library were more significant than those in JEFF 3.1, JENDL 3.3, and ENDF/B-VII.0. This indicates that neutron capture by ^{238}Pu at JENDL 4.0 is lower than that at JEFF 3.1, JENDL 3.3, and ENDF/B-VII.0. Therefore, the number of ^{238}Pu in JENDL 4.0 at the end of reactor operation is higher than that in the other three libraries.

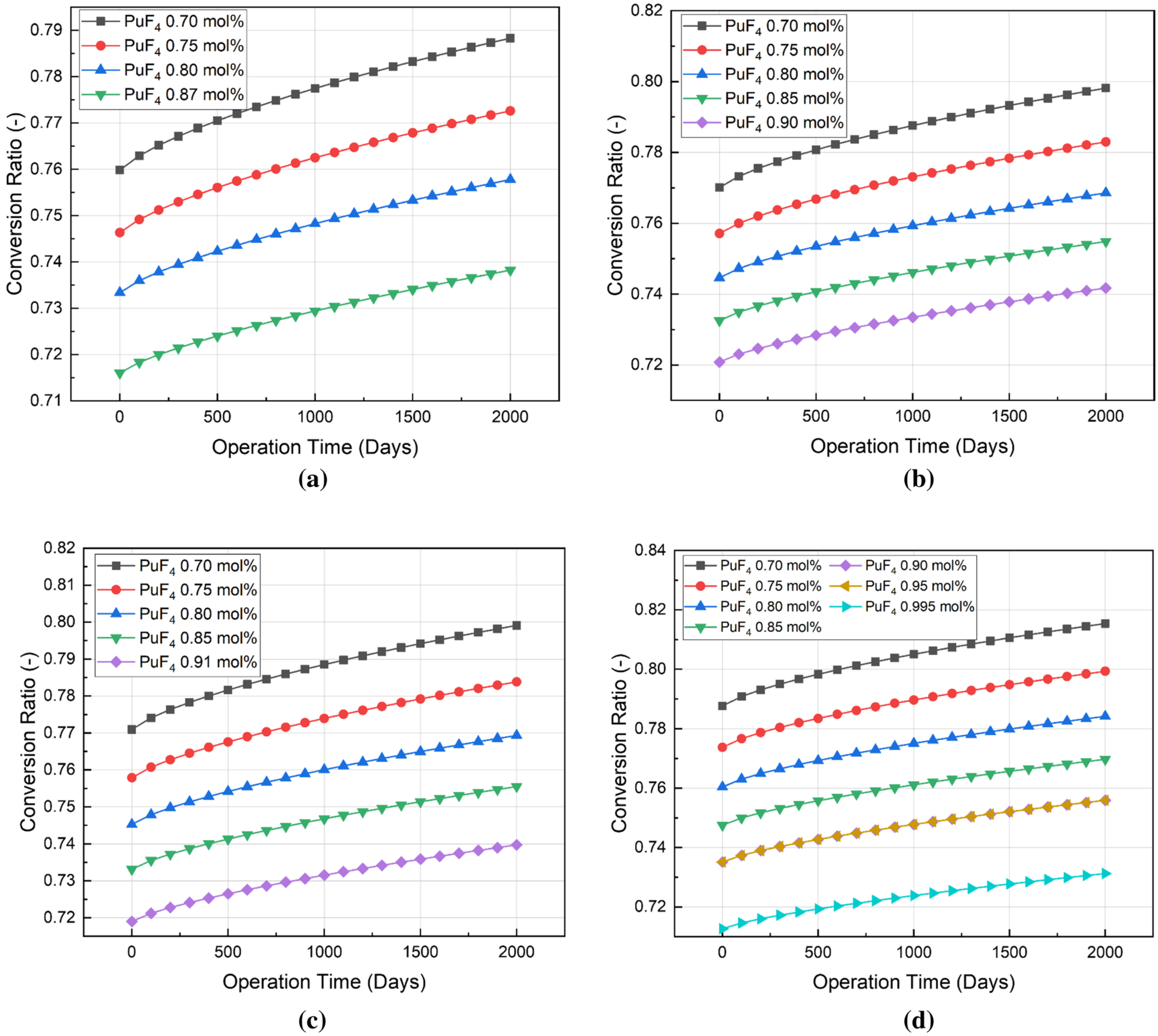

Fig. 8 (Color online) The conversion ratio with various concentrations of WGPu fuel for **a** JENDL 3.3, **b** JENDL 4.0, **c** ENDF/B-VII.0, and **d** JEFF 3.1

Figure 11 shows that the atomic density of ^{239}Pu decreases during operation time for all libraries used. The difference in the atomic density of ^{239}Pu is not significantly different in all libraries used. However, the reduction in the atomic density of ^{239}Pu in JENDL 3.3 is more significant than that of ENDF/B-VII.0, JEFF 3.1, and JENDL 4.0 (Table 13). It indicates that the fission rate of ^{239}Pu is higher in JENDL 3.3 compared to in the other three libraries. It may affect the higher k_{eff} value in the JENDL 3.3 library, as shown in Fig. 3.

Figure 12 shows the change in the atomic density of ^{241}Am during reactor operation for different nuclear data libraries. The change in the JEFF 3.1 library is lower than that in the ENDF/B-VII and JENDL libraries. This means that the conversion process of ^{241}Am, either through fission reactions or transmutation in JEFF 3.1, occurs more frequently than in the other three libraries. Therefore, it may cause the conversion capability in JEFF 3.1 to become higher than that of the other libraries. This difference could also be due to the different conversion rates of ^{241}Pu, which then produces ^{241}Am in the reactor.

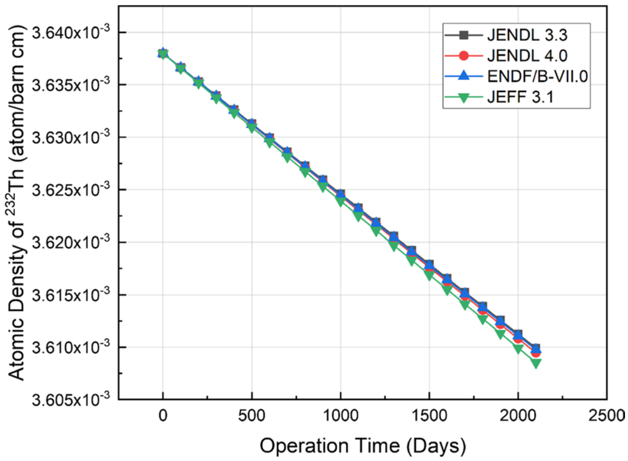

Fig. 9 (Color online) The change of ^{232}Th atomic density for different nuclear data libraries

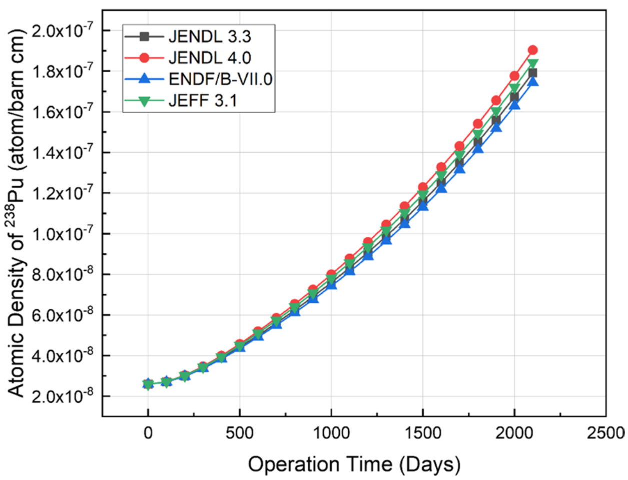

Fig. 10 (Color online) The change in ^{238}Pu atomic density for different nuclear data libraries

4.3 Effect of the nuclear data library on the neutron spectrum

The neutron spectrum, which describes the neutron flux distribution in the reactor core based on the energy range, is another significant parameter in nuclear reactor studies. In this analysis, the neutron spectrum was explained by the relative flux per unit lethargy, which is the neutron flux multiplied by the neutron energy. For example, the spectrum of 0.80 mol% of the PuF_4 concentration with different nuclear data libraries as a function of energy at the beginning of a cycle of the reactor is depicted in Fig. 13, which shows for each region: (a) Core 1, (b) Core 2, and (c) Core 3. The neutron spectrum from each region exhibited a similar trend for all three nuclear data libraries. However, the neutron spectra in the thermal energy range

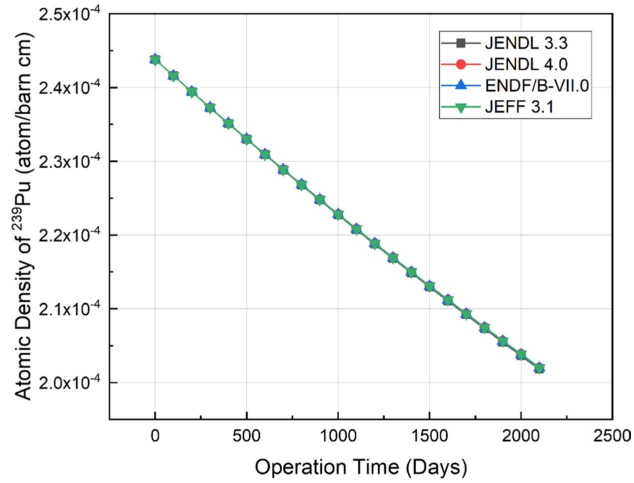

Fig. 11 (Color online) The change in ^{239}Pu atomic density for different nuclear data libraries

were lower than those in the fast energy range for all the core regions. In other words, the obtained neutron spectra were difficult to obtain in all regions of the reactor core. This is due to the high eta value of the loaded plutonium in the fast energy range, which is defined as the ratio of the total generated neutrons to the total absorbed neutrons in the reactor core.

In the thermal energy range, the neutron spectrum for JENDL 3.3 is the highest, followed by that for ENDF/B-VII.0, JEFF 3.1, and JENDL 4.0. This is because of the higher capture cross section of ^{232}Th and ^{238}Pu in JENDL 3.3 than in JENDL 4.0 [19]. For comparison, the neutron spectrum in the thermal energy range for Core 2 is shown in Fig. 14. This shows that the neutron spectra in ENDF/B-VII.0 and JEFF 3.1 are more thermalized than those in JENDL 4.0. Therefore, there is an overestimated value for ENDF/B-VII.0 and JEFF 3.1. Because ^{239}Pu is used as the main fissile in this reactor and is also a superior fissile in the fast energy range, the obtained k_{eff} values in ENDF/B-VII.0 and JEFF 3.1 are lower than those in JENDL 4.0, as shown in Fig. 3.

Moreover, the thermal peak in the Core 2 region was the highest, followed by that in the Core 1 or 3 region. For instance, Fig. 15 compares the neutron spectra of all regions for JENDL 4.0. This result is due to the large moderator fraction utilized in the Core 2 region, which impacts the moderating process of fast neutrons into thermal neutrons. Consequently, the number of moderators utilized in the active core is proportional to the peak of the neutron spectrum in the thermal energy range. Furthermore, the impact of the peaks of the radiative neutron capture cross section and fission cross section of ^{233}U, ^{239}Pu, and ^{241}Pu at 1 eV energy is predicted to induce the peak neutron spectrum in the thermal energy range.

Table 13 Atomic density of ^{239}Pu (atom/barn cm) during operation time

Time (Days)	JENDL 3.3	JENDL 4.0	ENDF/B-VII.0	JEFF 3.1
0	2.43797×10^{-4}	2.43797×10^{-4}	2.43797×10^{-4}	2.43797×10^{-4}
400	2.35112×10^{-4}	2.35146×10^{-4}	2.35130×10^{-4}	2.35134×10^{-4}
800	2.26778×10^{-4}	2.26851×10^{-4}	2.26819×10^{-4}	2.26833×10^{-4}
1200	2.18771×10^{-4}	2.18887×10^{-4}	2.18840×10^{-4}	2.18866×10^{-4}
1600	2.11067×10^{-4}	2.11228×10^{-4}	2.11166×10^{-4}	2.11209×10^{-4}
2000	2.03644×10^{-4}	2.03852×10^{-4}	2.03776×10^{-4}	2.03838×10^{-4}

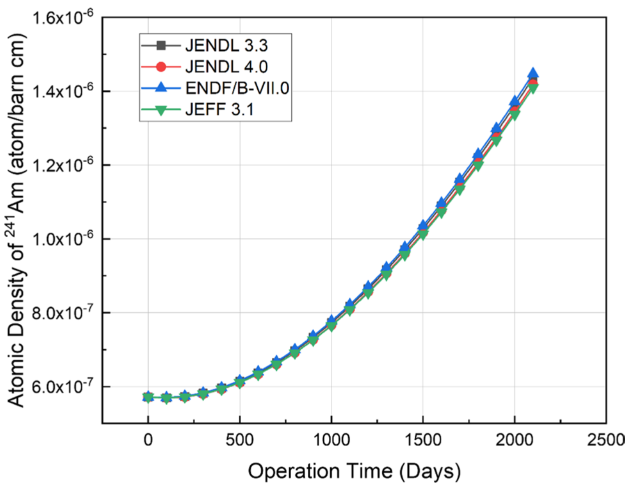

Fig. 12 (Color online) The change in the ^{241}Am atomic density for different nuclear data libraries

As shown in Fig. 16, increasing the PuF_4 concentration also affected the neutron spectrum, especially in the thermal energy range. In addition, the obtained neutron spectrum becomes harder with increasing PuF_4 concentration, owing to the higher total plutonium utilized in the fuel salt.

4.4 Safety parameter analysis (MTC, DRC, and CRW)

Regarding the safety aspect, several safety parameters, such as MTC, DRC, and CRW, were analyzed to determine the minimal PuF_4 concentration required in the reactor. Figure 17 shows the change in reactor reactivity as a function of moderator temperature for the four different nuclear libraries. The moderator temperature was varied from 800 to 1200 K. The reactivity value decreased with increasing moderator temperature for all nuclear libraries. The MTC value was examined based on the ratio of the reactor reactivity change to the moderator temperature change. In this case, the MTC values for all nuclear libraries were negative, as shown in Table 12.

Figure 18 depicts the reactor reactivity as a function of temperature for the four nuclear libraries, in which the reactivity values decreased with increasing temperature. The temperature was varied from 800 to 1200 K. The DRC value could be evaluated based on the ratio of the reactor reactivity change to temperature change. As shown in Table 12, the DRC values of the reactors were negative for all the nuclear libraries. This shows that the reactor with the minimal PuF_4 concentration required had inherent safety criteria. In accordance with the present results, previous studies have demonstrated that the temperature coefficient must be negative [35, 36].

In addition, the CRW value was analyzed, which is defined as the subtraction of the reactor reactivity without a control rod and the reactivity with control rod insertion. In this study, several control rod distribution models were varied. In Model 1, the reactor was calculated without a control rod, whereas in Model 2, the reactor was equipped with control rod 1. Model 3 was designed with control rods 1 and 2, whereas Model 4 was arranged using control rods 1, 2, and 3, as shown in Fig. 19. The control rod was B_4C (90% boron-enriched) [37]. In this study, the CRW value was calculated for the minimal PuF_4 concentration required for the JENDL 4.0 library. As presented in Table 13, the initial k_{eff} and reactivity of Model 1 were the highest, followed by those of Model 2, 3, and 4, because of the lowest neutron absorption in Model 1. The CRW value of Model 4 was the highest, followed by that of Model 3 and 2, owing to the significant number of control rods utilized in the reactor. As a common feature, the reactivity of the reactor decreased with an increase in the control rod amount in the reactor (Tables 14 and 15).

5 Conclusion

A study evaluating the JEFF 3.1, JENDL 3.3, ENDF/B-VII.0, and JENDL 4.0 nuclear data libraries for a small 100 MWe MSR with plutonium fuel was conducted. The variation in the PuF_4 concentration in the reactor core affected some parameters, such as criticality, conversion

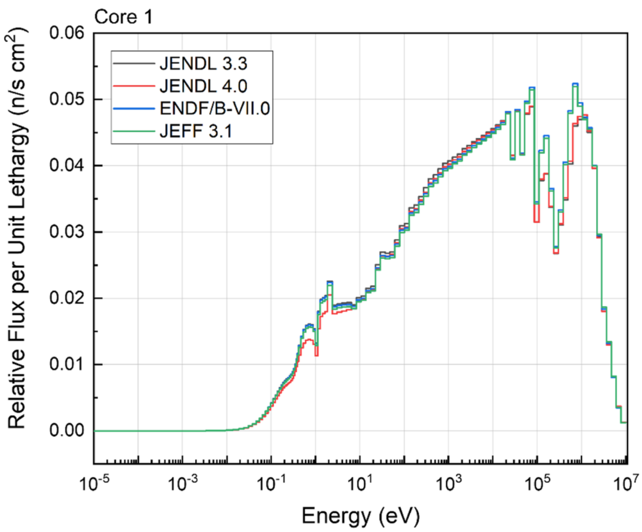

(a)

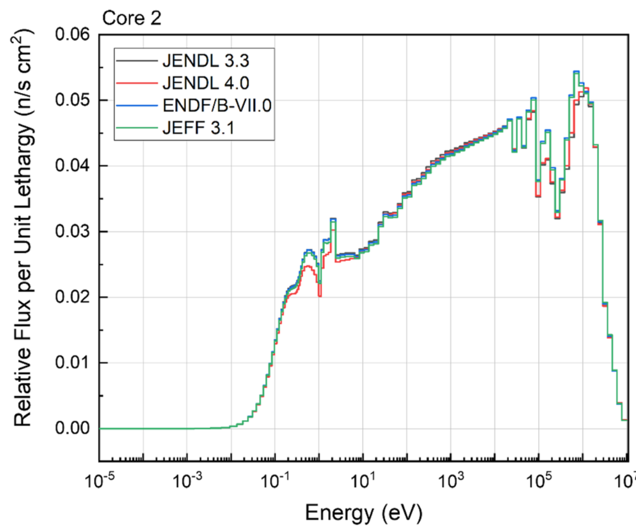

(b)

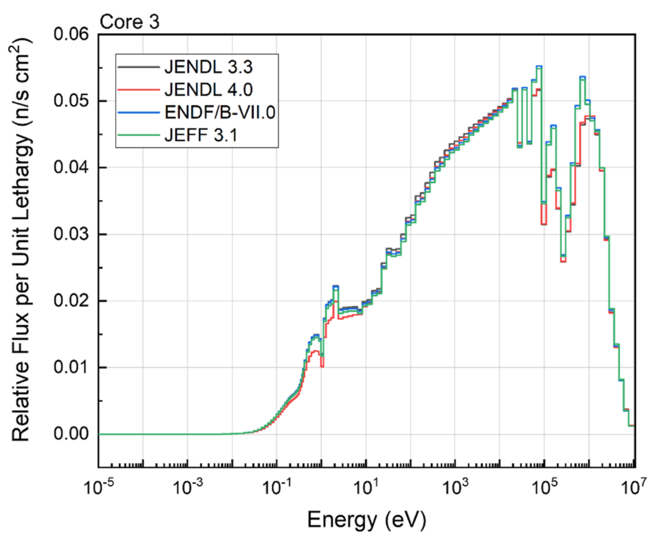

(c)

Fig. 13 (Color online) Comparison of the neutron spectrum with WGPu fuel of 0.80%mol for all regions: **a** Core 1, **b** Core 2, and **c** Core 3

capability, and neutron spectra. In the criticality analysis, the k_{eff} value increased with the increase in PuF_4 concentration, and this value diminished with operation time. The reactor can be operated in critical conditions with the minimum concentration of PuF_4 fuel loaded of about 0.995 mol% for JEFF 3.1, 0.91 mol% for ENDF/B-VII.0, 0.90 mol% for JENDL 4.0, and 0.87 mol% for JENDL 3.3. The diverse obtained values of the evaluated parameters show trans-plutonium's sensitivity with different nuclear data libraries. The obtained results also show that the reactor can burn at least as much plutonium fuel as the minimum concentration of PuF_4 required to achieve reactor criticality. The CR decreased with increasing PuF_4 concentration, and this parameter increased with operating time. When comparing the neutron spectra in the Core 1, 2, and 3 areas, it is clear that the fuel volume fraction impacts the

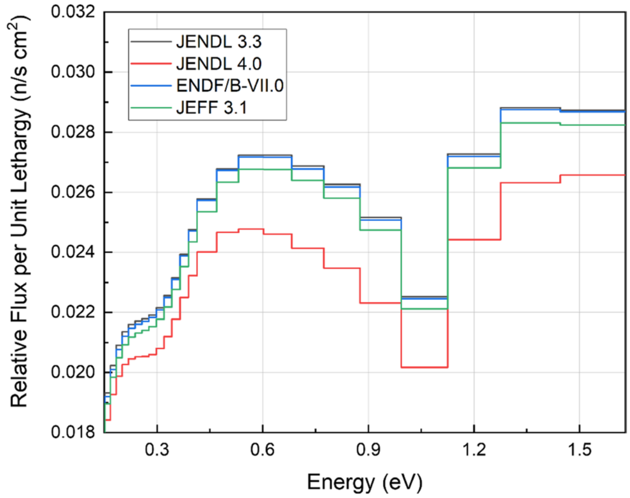

Fig. 14 (Color online) Comparison of the neutron spectrum of the Core 2 region in the thermal energy range

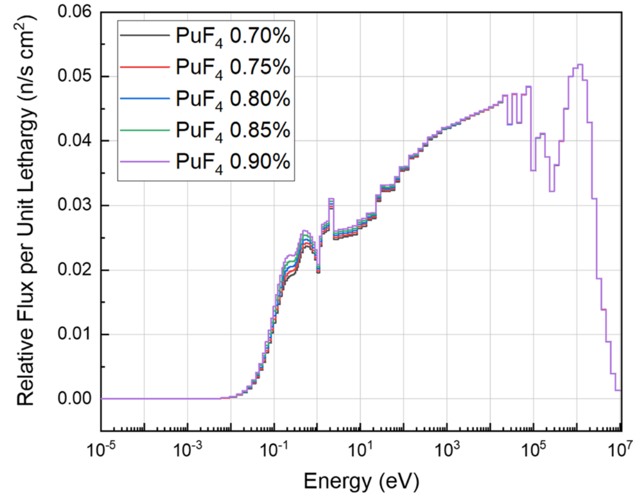

Fig. 16 (Color online) Comparison of the neutron spectrum for several PuF_4 concentrations in the Core 2 region with JENDL 4.0

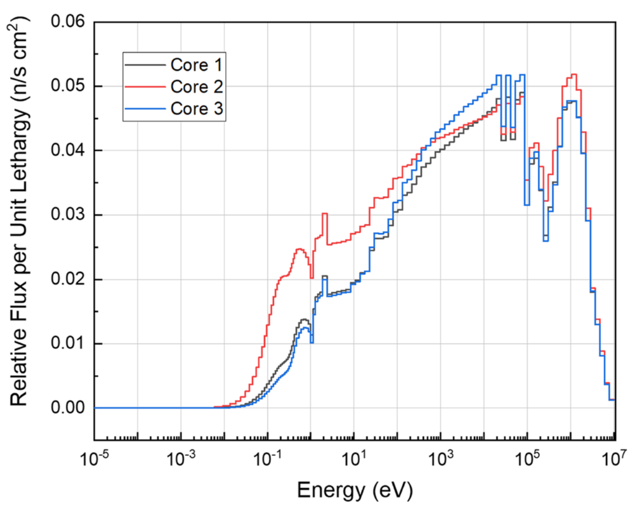

Fig. 15 (Color online) Comparison of the neutron spectrum in all region cores for JENDL 4.0

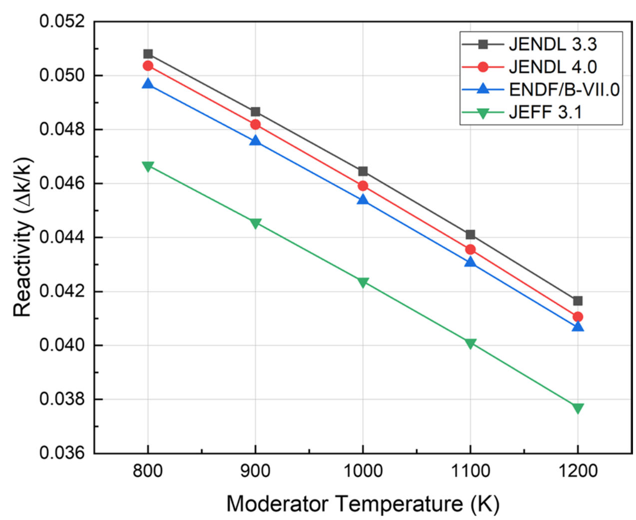

Fig. 17 (Color online) The reactivity with different moderator temperatures for JENDL 3.3, JENDL 4.0, ENDF/B-VII.0, and JEFF 3.1

neutron distribution, which becomes more difficult as the fuel volume fraction increases. The results obtained from all nuclear data libraries have different values, and JENDL 4.0 is more representative of the neutronic calculation results of the small MSR. Based on the obtained neutron spectrum in Core 2 in the thermal energy range, for JENDL 4.0, JENDL 3.3, JEFF 3.1, and ENDF/B-VII.0, there were some overestimated cross-section values in JENDL 3.3, JEFF 3.1, and ENDF/B-VII.0. In the safety analysis, the MTC and DRC values were negative for the minimum concentration PuF_4 required case, which demonstrated that the reactor had an inherent safety feature. The B_4C control rod insertion in the reactor had an impact on the reactor reactivity and CRW value, in which the reactivity decreased and the CRW value increased.

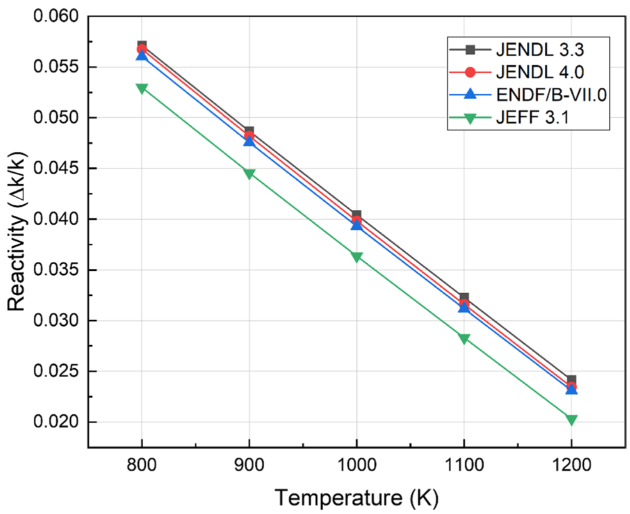

Fig. 18 (Color online) The reactivity with different temperatures for JENDL 3.3, JENDL 4.0, ENDF/B-VII.0, and JEFF 3.1

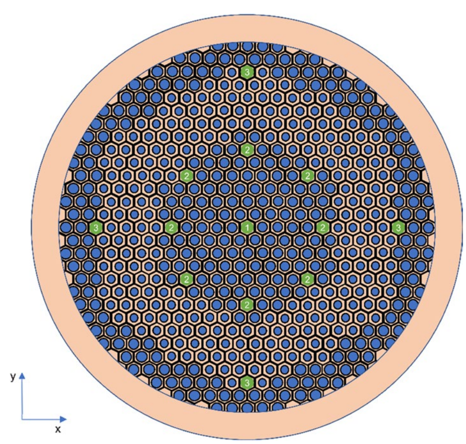

Fig. 19 (Color online) Control rod distribution in the reactor

Table 14 Moderator temperature coefficient (MTC) and Doppler reactivity coefficient (DRC) values of the reactor for different nuclear libraries

Nuclear Libraries	JENDL 3.3	JENDL 4.0	ENDF/B-VII.0	JEFF 3.1
MTC (pcm/K)	−2.34	−2.37	−2.30	−2.28
DRC (pcm/K)	−8.17	−8.24	−8.15	−8.08

Table 15 Initial k_{eff}, reactivity, and Doppler reactivity coefficient (DRC) values for different reactor models

Coefficient	Model 1	Model 2	Model 3	Model 4
Initial k_{eff}	1.0530	1.0491	0.9964	0.9829
Reactivity ($\Delta k/k$)	0.00503	0.0468	−0.0036	−0.0174
DRC (pcm/K)	–	349.40	5395.77	6777.93

Author contributions All authors contributed to the study conception and design. Data collection and analysis were performed by Cici Wulandari, Abdul Waris, Sidik Permana, and Syeilendra Pramuditya. The first draft of the manuscript was written by Cici Wulandari and all authors commented on previous versions of the manuscript. All authors read and approved the final manuscript.

References

1. J.C. Gehin, J.J. Powers, Liquid fuel molten salt reactors for thorium utilization. Nucl. Technol. **194**, 152 (2016). https://doi.org/10.13182/NT15-124
2. E.S. Bettis, W.B. Cottrell, E.R. Mann et al., The aircraft reactor experiment—operation. Nucl. Sci. Eng. **2**, 841–853 (1957). https://doi.org/10.13182/NSE57-A35497
3. W.K. Ergen, A.D. Callihan, C.B. Mills et al., The aircraft reactor experiment—physics. Nucl. Sci. Eng. **2**, 826–840 (1957). https://doi.org/10.13182/NSE57-A35496
4. P. Haubenreich, J. Engel, Experience with the molten-salt reactor experiment. Nucl. Appl. Technol. **8**, 118–136 (1970). https://doi.org/10.13182/NT8-2-118
5. J. Park, Y. Jeong, H.C. Lee et al., Whole core analysis of molten salt breeder reactor with online fuel reprocessing. Int. J. Energy Res. **39**, 1673–1680 (2015). https://doi.org/10.1002/er.3371
6. L. Mathieu, D. Heuer, R. Brissot et al., The thorium molten salt reactor: moving on from the MSBR. Prog. Nucl. Energ. **48**, 664–679 (2006). https://doi.org/10.1016/j.pnucene.2006.07.005
7. A. Nuttin, D. Heuer, A. Billebaud et al., Potential of thorium molten salt reactorsdetailed calculations and concept evolution with a view to large scale energy production. Prog. Nucl. Energ. **46**, 77–99 (2005). https://doi.org/10.1016/j.pnucene.2004.11.001
8. K. Furukawa, K. Arakawa, L.B. Erbay et al., A road map for the realization of global-scale thorium breeding fuel cycle by single molten-fluoride flow. Energ. Convers. Manag. **49**, 1832–1848 (2008). https://doi.org/10.1016/j.enconman.2007.09.027
9. K. Furukawa, L.B. Erbay, A. Aykol, A study on a symbiotic thorium breeding fuel-cycle: THORIMS-NES through FUJI. Energ. Convers. Manag. **63**, 51–54 (2012). https://doi.org/10.1016/j.enconman.2012.01.030
10. K. Mitachi, T. Yamamoto, R. Yoshioka, Three-region core design for 200-MW(electric) molten-salt reactor with thorium-uranium fuel. Nucl. Technol. **158**, 348–357 (2007). https://doi.org/10.13182/NT07-A3846
11. S.Q. Jaradat, A.B. Alajo, Studies on the liquid fluoride thorium reactor: comparative neutronics analysis of MCNP6 code with SRAC95 reactor analysis code based on FUJI-U3-(0). Nucl. Eng. Des. **314**, 251–255 (2017). https://doi.org/10.1016/j.nucengdes.2017.02.013
12. K. Furukawa, Y. Kato, S.E. Chigrinov, Plutonium (TRU) transmutation and 233U production by single-fluid type accelerator molten-salt breeder (AMSB). AIP. Conf. Proc. **346**, 745–751 (1995). https://doi.org/10.1063/1.49112
13. Y. Honma, Y. Shimazu, T. Narabayashi, Optimization of flux distribution in a molten-salt reactor with a 2-region core for plutonium burning. Prog. Nucl. Energ. **50**, 257–261 (2008). https://doi.org/10.1016/j.pnucene.2007.11.073
14. X. Zhou, Z.H. Liu, C. Chen et al., Real-time wide-range neutron flux monitor for thorium-based molten salt reactor. Nucl. Sci. Tech. **29**, 107 (2018). https://doi.org/10.1007/s41365-018-0450-9
15. C. Wulandari, A. Waris, S. Pramuditya et al., Study on utilization of super grade plutonium in molten salt reactor FUJI-U3 using

CITATION code. J. Phys. Conf. Ser. **877**, 012021 (2017). https://doi.org/10.1088/1742-6596/877/1/012021
16. C. Wulandari, A. Waris, S. Permana et al., Plutonium and minor actinides utilization in FUJI-U1 molten salt reactor. J. Phys. Conf. Ser. **1204**, 012132 (2019). https://doi.org/10.1088/1742-6596/1204/1/012132
17. A. Waris, V. Richardina, I.K. Aji et al., Preliminary study on plutonium and minor actinides utilization in thorims-nes minifuji reactor. Energ. Convers. Manag. **72**, 27–32 (2013). https://doi.org/10.1016/j.enconman.2013.03.005
18. A. Waris, I.K. Aji, S. Pramuditya et al., Preliminary study on LiF4-ThF4-PuF4 utilization as fuel salt of miniFUJI molten salt reactor. J. Phys. Conf. Ser. **739**, 012004 (2016). https://doi.org/10.1088/1742-6596/739/1/012004
19. T. Nakagawa, K. Shibata, S. Chiba et al., Japanese evaluated nuclear data library version 3 revision-2: JENDL-3.2. J. Nucl. Sci. Technol. **32**, 1259–1271 (1995). https://doi.org/10.1080/18811248.1995.9731849
20. K. Shibata, T. Kawano, T. Nakagawa et al., Japanese evaluated nuclear data library version 3 revision-3: JENDL-3.3. J. Nucl. Sci. Technol. **39**, 1125–1136 (2002). https://doi.org/10.1080/18811248.2002.9715303
21. K. Shibata, O. Iwamoto, T. Nakagawa et al., JENDL-4.0: a new library for nuclear science and engineering. J. Nucl. Sci. Technol. **48**, 1–30 (2011). https://doi.org/10.1080/18811248.2011.9711675
22. D.Y. Cui, S.P. Xia, X.X. Li et al., Transition toward thorium fuel cycle in a molten salt reactor by using plutonium. Nucl. Sci. Tech. **28**, 152 (2017). https://doi.org/10.1007/s41365-017-0303-y
23. P. Yang, Z.K. Lin, W. Wan et al., Preliminary neutron study of a thorium-based molten salt energy amplifier. Nucl. Sci. Tech. **31**, 41 (2020). https://doi.org/10.1007/s41365-020-0750-8
24. Y. Zhong, X. Yang, D. Ding et al., Numerical study of the dynamic characteristics of a single-layer graphite core in a thorium molten salt reactor. Nucl. Sci. Tech. **29**, 141 (2018). https://doi.org/10.1007/s41365-018-0488-8
25. C.Y. Li, X.B. Xia, J. Cai et al., Radiation dose distribution of liquid fueled thorium molten salt reactor. Nucl. Sci. Tech. **32**, 22 (2021). https://doi.org/10.1007/s41365-021-00857-3
26. W.M. Stacey, *Nuclear Reactor Physics*, 2nd edn. (Wiley, New York, 2004)
27. B. Pellaud, Proliferation aspects of plutonium recycling. Comptes. Rendus. Phys. **3**, 1067 (2002). https://doi.org/10.1016/S1631-0705(02)01364-6
28. J. Wu, Y. Ma, C. Yu et al., Nuclear non-proliferation review and improving proliferation resistance assessment in the future. Int. J. Energy Res. (2021). https://doi.org/10.1002/er.5486
29. A. Koning, R. Forrest, M. Kellett et al., *The JEFF-31 nuclear data library—JEFF report 21* (Nuclear Energy Agency-Organisation for Economic Co-Operation and Development, France, 2006)
30. M.B. Chadwick, P. Obložinský, M. Herman et al., ENDF/B-VII.0: next generation evaluated nuclear data library for nuclear science and technology. Nucl. Data Sheets **107**, 2931 (2006). https://doi.org/10.1016/j.nds.2006.11.001
31. G. Zhu, W. Guo, X. Kang et al., Neutronic effect of graphite dimensional change in a small modular molten salt reactor. Int. J. Energy Res. **45**, 11976–11991 (2021). https://doi.org/10.1002/er.5964
32. R.R. Romatoski, L.W. Hu, Fluoride salt coolant properties for nuclear reactor applications: a review. Ann. Nucl. Energy **109**, 635–647 (2017). https://doi.org/10.1016/j.anucene.2017.05.036
33. Z. Guo, C. Wang, D. Zhang et al., The effects of core zoning on optimization of design analysis of molten salt reactor. Nucl. Eng. Des. **265**, 967–977 (2013). https://doi.org/10.1016/j.nucengdes.2013.09.036
34. K. Nagy, J.L. Kloosterman, D. Lathouwers et al., The effects of core zoning on the graphite lifespan and breeding gain of a moderated molten salt reactor. Ann. Nucl. Energy **43**, 19–25 (2012). https://doi.org/10.1016/j.anucene.2011.12.025
35. Y.P. Zhang, Y.W. Ma, J.H. Wu et al., Preliminary analysis of fuel cycle performance for a small modular heavy water-moderated thorium molten salt reactor. Nucl. Sci. Tech. **31**, 108 (2020). https://doi.org/10.1007/s41365-020-00823-5
36. X.X. Li, Y.W. Ma, C.G. Yu et al., Effects of fuel salt composition on fuel salt temperature coefficient (FSTC) for an under-moderated molten salt reactor (MSR). Nucl. Sci. Tech. **29**, 110 (2018). https://doi.org/10.1007/s41365-018-0458-1
37. O. Ashraf, A. Rykhlevskii, G.V. Tikhomirov et al., Preliminary design of control rods in the single-fluid double-zone thorium molten salt reactor (SD-TMSR). Ann. Nucl. Energy **152**, 108035 (2021). https://doi.org/10.1016/j.anucene.2020.108035

Springer Nature or its licensor (e.g. a society or other partner) holds exclusive rights to this article under a publishing agreement with the author(s) or other rightsholder(s); author self-archiving of the accepted manuscript version of this article is solely governed by the terms of such publishing agreement and applicable law.